Reentrant behaviour in Y-doped $Ho_{0.75}Y_{0.25}Ni_2B_2C$ single crystal

2006 J. Phys.: Condens. Matter 18 8533

(http://iopscience.iop.org/0953-8984/18/37/011)

INSTITUTE OF PHYSICS PUBLISHING JOURNAL OF PHYSICS: CONDENSED MATTER

J. Phys.: Condens. Matter **18** (2006) 8533–8539 doi:10.1088/0953-8984/18/37/011

Reentrant behaviour in Y-doped $Ho_{0.75}Y_{0.25}Ni_2B_2C$ single crystal

S R Zhao[1], **Z A Xu**[1,4], **H Takeya**[2], **K Hirata**[2] **and J L Luo**[3]

[1] Department of Physics, Zhejiang University, Hangzhou 310027, People's Republic of China
[2] National Institute for Materials Science, 1-2-1 Sengen, Tsukuba, Ibaraki 305-0047, Japan
[3] Beijing National Laboratory for Condensed Matter Physics, Institute of Physics, Chinese Academy of Sciences, Beijing 100080, People's Republic of China

E-mail: zhuan@zju.edu.cn

Received 24 February 2006, in final form 17 July 2006
Published 1 September 2006
Online at stacks.iop.org/JPhysCM/18/8533

Abstract
The transport and superconducting properties of $Ho_{0.75}Y_{0.25}Ni_2B_2C$ single crystals were investigated to study the competing effects between superconductivity and magnetism. The superconducting transition temperature T_c is 7.6 K, determined from the resistivity transition; meanwhile, the commensurate antiferromagnetic (AFM) transition occurs at T_N of 3.9 K, which is lower than that of pure $HoNi_2B_2C$ ($T_N \approx 5$ K). $Ho_{0.75}Y_{0.25}Ni_2B_2C$ reentered into the normal state at T_m ($T_N < T_m < T_c$) when small magnetic fields were applied along the crystallographic c-axis. In contrast to the case in $HoNi_2B_2C$, the reentrant behaviour for $Ho_{0.75}Y_{0.25}Ni_2B_2C$ only appears when the applied field H is along the c-axis, and the reentrant peak position $T_P(H)$ shifts to lower temperature with increasing applied field. We suggest that the disorder of magnetic structure induced by Y doping may account for the significant difference in the reentrant behaviour between $Ho_{0.75}Y_{0.25}Ni_2B_2C$ and $HoNi_2B_2C$. Moreover, there does not exist a deep minimum in the upper critical field $H_{c2}(T)$ line at T_N of 3.9 K for either $H \parallel c$ or $H \perp c$. The H–T phase diagram is derived and discussed.

1. Introduction

The recently discovered rare-earth nickel boride carbides, RNi_2B_2C (R = rare-earth elements, Y and Sc) have attracted a lot of attention because of their high superconducting transition temperatures among bulk intermetallic compounds [1–4], abundant magnetic phase diagrams [4–9] and coexistence of superconducting order and magnetic order [3–7, 10–14]. Among the RNi_2B_2C family, magnetic borocarbide superconductors (Ho, Dy, Tm, Er)Ni_2B_2C exhibit the destruction of superconductivity and reenter the normal state below the superconducting transition temperature T_c under applied field; then the superconducting state

[4] Author to whom any correspondence should be addressed.

is restored below the commensurate antiferromagnetic (AFM) transition temperature T_N. This kind of magnetic ordering induced reentrant behaviour has been discussed in the literature [4]. All the existing experimental results of the above four members strongly indicate that the superconducting reentrant transition temperature is almost the same as the AFM transition temperature T_N, and there exists a deep minimum in the upper critical field $H_{c2}(T)$ at T_N due to the destruction of superconductivity induced by the magnetic ordering. For example, in the case of $HoNi_2B_2C$, the reentrant behaviour has been observed for the applied field H both parallel and perpendicular to the c-axis [4, 7, 10–15], and the reentrant resistance peak locates at T_N of about 5 K, and there exists a deep minimum in $H_{c2}(T)$ around T_N. Moreover, incommensurate spiral magnetic structures in $HoNi_2B_2C$ were observed below a certain temperature T_m ($T_m > T_N$) and a metamagnetic transition from the spiral magnetic state to the commensurate AFM state happens at T_N. It is suggested that the metamagnetic transition may account for the behaviour of $H_{c2}(T)$ and thus the reentrance of superconductivity [7, 16].

The effects of nonmagnetic impurities on the reentrant behaviour of magnetic borocarbide superconductors have been studied on polycrystalline $Y_{1-x}Ho_xNi_2B_2C$ samples [10, 17], which show similar reentrant behaviour in resistivity to that of $HoNi_2B_2C$ [11, 13]. However, Lu-doped $Er_{0.8}Lu_{0.2}Ni_2B_2C$ single crystal does not exhibit reentrant behaviour [18]. Because of the significant anisotropy in the magnetic properties of Ho(Er, Tb) Ni_2B_2C samples, single crystals are necessary to study the competing effects between magnetism and superconductivity as well as the doping effect of nonmagnetic rare-earth elements on the magnetic ordering and the reentrant behaviour.

In this study, Y-doped $Ho_{0.75}Y_{0.25}Ni_2B_2C$ single-crystalline samples were synthesized, and the in-plane resistivity under different applied magnetic fields, and the specific heat were measured to study the effects of Y doping on the reentrant behaviour. The reentrance only appears as the applied field H is along the c-axis, and the reentrant peak $T_P(H)$ shifts to lower temperatures with increasing H. No deep minimum in the upper critical field $H_{c2}(T)$ is observed. The H–T phase diagram is derived and discussed. We suggest that the disorder of magnetic structure induced by Y doping may account for the significant difference in the reentrant behaviour between $Ho_{0.75}Y_{0.25}Ni_2B_2C$ and $HoNi_2B_2C$.

2. Experimental details

$Ho_{0.75}Y_{0.25}Ni_2B_2C$ single crystal was grown by the floating-zone technique. Details of the sample growth have been reported elsewhere [19]. The x-ray diffraction (XRD) pattern of the crushed powder was obtained at room temperature. All the XRD peaks can be indexed to the tetragonal $HoNi_2B_2C$ phase and no impurity peaks were observed, indicating a good sample quality. Chemical analysis by energy dispersive of x-ray (EDX) microanalysis was performed on an EDAX GENESIS 4000 x-ray analysis system affiliated to a scanning electron microscope (SEM, model SIRION), and an area averaging of two 1 mm^2 spots was performed. The atom number ratio of Ho^{3+}:Y^{3+} determined by EDX analysis is 71:29, which is close to the nominal atom number ratio 3:1. A standard four-probe method was used to measure the in-plane resistivity. The sample for the resistivity measurement was about 3 mm long (along the a- or b-axis direction), 1 mm wide and 0.3 mm thick (along the c-axis direction), and an ac current of 10 mA was applied along the a- or b-axis direction. The current dependence of the magneto-resistivity was also checked near the reentrant peak. All the measurements were performed on a Quantum Design PPMS-9 system and the magnetic field was applied both parallel and perpendicular to the crystallographic c-axis. The upper critical field (H_{c2}) was determined in each case from the magneto-resistivity curves using a criterion of 90% of the normal resistivity.

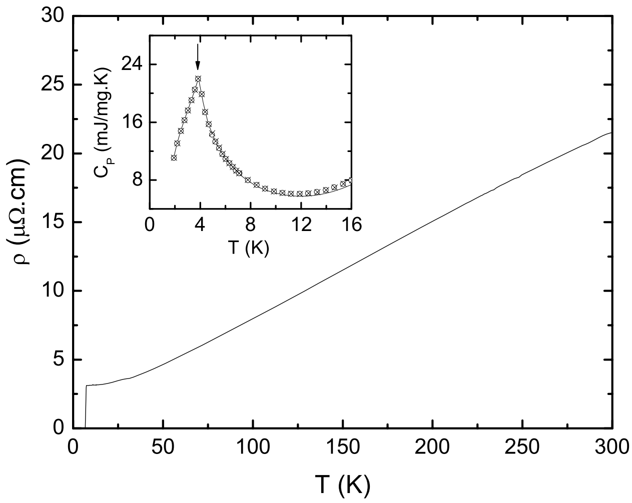

Figure 1. Temperature dependence of in-plane resistivity at zero applied field. The zero point of the superconducting transition temperature is 7.6 K. Inset: temperature dependence of specific heat under different applied magnetic fields along the *c*-axis. The line stands for zero applied field, the × symbols stand for $H = 2$ kOe, and the open circles stand for $H = 5$ kOe. The λ-peak at 3.9 K is due to the AFM transition.

3. Results and discussion

Figure 1 shows the temperature dependence of the in-plane resistivity for the temperature range from 2 to 300 K at zero applied field. The zero point of superconducting transition temperature is 7.6 K, and the transition width is less than 0.5 K. The high-temperature (200 K to room temperature) resistivity is linear with temperature, just like in other RNi_2B_2C family members [20, 21]. The inset of figure 1 shows the low-temperature specific heat versus temperature under different applied fields along the *c*-axis, which reveals a commensurate AFM transition temperature T_N of about 3.9 K. The specific heat was measured for $H = 0$, 1, 1.5, 2 and 5 kOe, but only the data for $H = 0$, 2 and 5 kOe are shown in the inset of figure 1 since the data for $H = 1$ and 1.5 kOe show almost the same λ-peak. This result means that T_N does not change with applied field H.

Figure 2 shows the applied field (H) dependence of the in-plane resistivity for $\mathbf{H} \parallel c$ (a) and $\mathbf{H} \perp c$ (b) at selected temperatures. The inset of figure 2(b) shows a comparison of the in-plane resistivity versus H at 5 K for $\mathbf{H} \parallel c$ and $\mathbf{H} \perp c$. For $\mathbf{H} \parallel c$, the reentrant behaviour is observed for the temperature range between 4 and 6.5 K. We define H_m as the onset point at which the resistivity starts to reenter into normal state, and H_P as the reentrant peak position in the resistivity. Both H_m and H_P increase with decreasing temperature. From these iso-temperature magneto-resistivity curves the upper critical magnetic field H_{c2} versus T is also derived. There is a significant difference in the iso-temperature magneto-resistivity curves between $Ho_{0.75}Y_{0.25}Ni_2B_2C$ and $HoNi_2B_2C$ single crystal [13]. First, the reentrant peak in $\rho(H)$ appears at temperatures higher than T_N and the peak position (H_P) changes with temperature. Second, H_{c2} increases monotonically with decreasing temperature, which means that there is no minimum in $H_{c2}(T)$ around T_N. Third, as the applied field H is perpendicular to the *c*-axis direction, no re-entrant behaviour in the in-plane resistivity is observed. The peak in resistivity at H_P has a saturation value of around 1.25 $\mu\Omega$ cm, which is still much lower than the normal state resistivity of 3.09 $\mu\Omega$ cm.

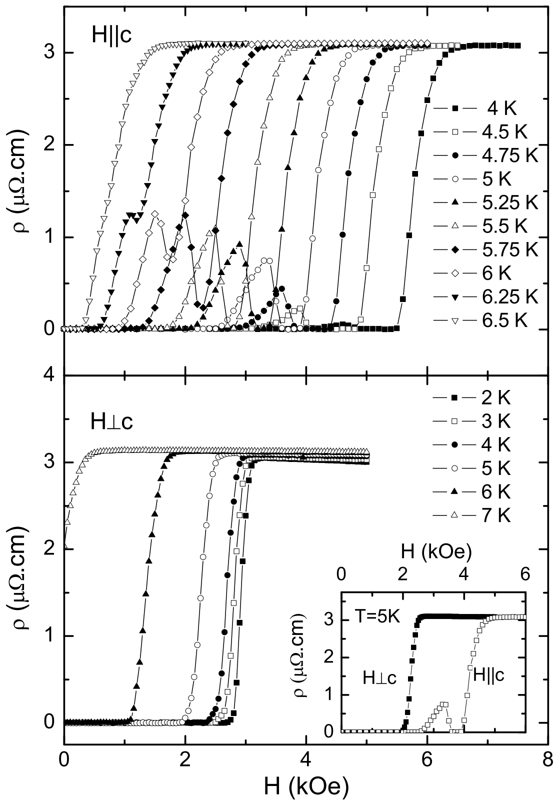

Figure 2. Plot of the in-plane resistivity as a function of applied field for $\mathbf{H} \parallel c$ (upper panel) and $\mathbf{H} \perp c$ (lower panel). The inset in the lower panel shows a comparison plot of the in-plane resistivity versus H at $T = 5$ K for $H \parallel c$ and $H \perp c$.

In order to obtain more details about the reentrant behaviour, the temperature dependence of the in-plane resistivity under different applied fields was also measured. Figure 3 shows the in-plane resistivity as a function of temperature at selected magnetic fields which were applied along the c-axis. The current dependence of the reentrant behaviour under H of 1.7 kOe (along the c-axis) is shown in the inset of figure 3. The characteristic temperature $T_m(H)$ is defined as the onset point at which the resistivity starts to reenter into normal state, and $T_P(H)$ as the reentrant peak position in the resistivity. The iso-field curves resemble the iso-temperature curves in figure 2(a). First, the reentrant peak shifts to higher temperatures as the applied field decreases; second, the peak in the resistivity has the same saturation value of about 1.25 $\mu\Omega$ cm. The reentrant peak appears only when 1 kOe $< H <$ 2.5 kOe. Thus, the significant difference in the reentrant behaviour is also manifested in the temperature dependence of the in-plane resistivity at selected applied fields between Y-doped and pure $HoNi_2B_2C$ single crystal [13]. It should be noted that the position of the reentrant peaks shows very weak current dependence although the height increases with increasing current. A similar effect of applied current on the entrant behaviour was also observed in pure $HoNi_2B_2C$ single crystal [13].

Furthermore, we plot all the parameters $H_{c2}^{\parallel}(T)$, $H_P(T)$ and $H_m(T)$ in figure 4. We define $H_{c2}^{\parallel}$ and $H_{c2}^{\perp}$ as the upper critical magnetic fields for H along and normal to the c-axis respectively. The vertical dashed line represents the AFM transition temperature T_N which does not change with H. The inset of figure 4 shows $H_{c2}^{\perp}$ versus T. Apparently there is no

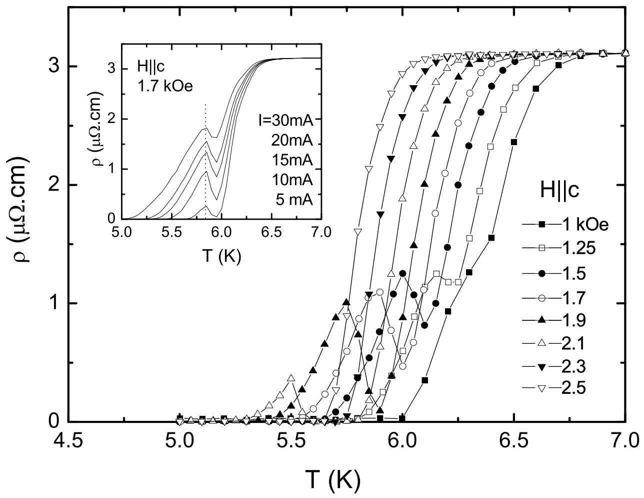

Figure 3. Temperature dependence of in-plane resistivity under selected magnetic fields along the *c*-axis. The reentrant peak appears in the field range between 1 and 2.5 kOe. Inset: a comparison of the resistivity versus temperature for different currents.

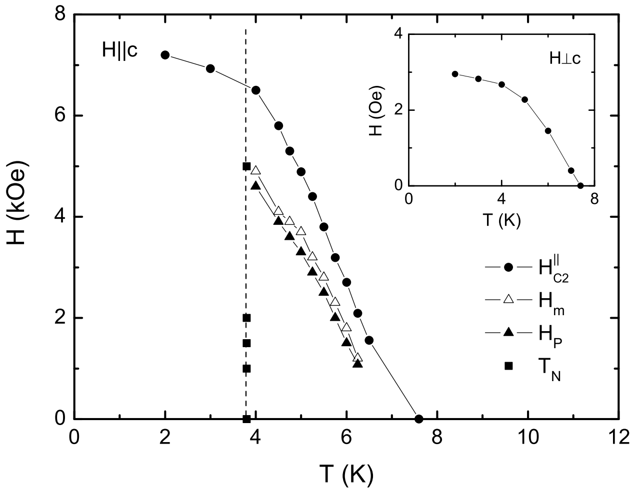

Figure 4. The H–T phase diagram for $\mathbf{H} \parallel c$. $H^{\parallel}_{c2}$, H_m, and H_P are described in the text; solid square, solid circle and solid triangle stand for the $H^{\parallel}_{c2}$, H_m, and H_P line respectively. The solid squares denote the commensurate AFM transition. Inset: $H^{\perp}_{c2}$ versus T.

deep minimum in either the $H^{\parallel}_{c2}(T)$ or the $H^{\perp}_{c2}(T)$ line around T_N. The reentrant region which is characterized by H_m and H_P only appears above T_N, in the temperature range between 4 and 6.5 K. The $H_m(T)$ and $H_P(T)$ lines scale with the $H^{\parallel}_{c2}(T)$ line. It is distinctively manifested in the H–T phase diagram that the reentrant peak does not occur simultaneously with the commensurate AFM transition, and the peak position T_P has a strong H dependence. All the above features are different from those of the $HoNi_2B_2C$ single crystal.

A minimum in the upper critical field $H_{c2}(T)$ around T_N has been commonly observed in antiferromagnetic superconductors such as RMo_6S_8 (R = Gd, Tb, and Dy) [22], $ErNi_2B_2C$ [6], and $HoNi_2B_2C$ [13]. Machida *et al* [23] studied the effect of the AFM molecular field on the

Cooper pairing and attributed the anomaly in $H_{c2}(T)$ to a reduction in the phase space (a phase space truncation induced by the AFM ordering). Takeya and Massalami [18] studied the effect of nonmagnetic substituents on the magnetism and superconductivity in $Er_{0.8}Lu_{0.2}Ni_2B_2C$ single crystal. They found that the nonmagnetic Lu doping causes the absence of the structure in $H_{c2}(T)$ at T_N and attributed it to an alloying-induced destruction of phase space truncation. We suggest that the absence of the minimum in $H_{c2}(T)$ in our study can also be attributed to the depression of the phase space truncation caused by Y doping. The decrease of T_N caused by Y doping is consistent with this scenario.

Meanwhile, the nonmagnetic substituent on the magnetic lattice can usually induce disorder in the magnetic structure and causes the long-range ordering of Ho^{3+} moments to be unstable. Neutron diffraction studies of $Ho_{1-x}Y_xNi_2B_2C$ polycrystalline samples have shown that Y doping severely suppresses the commensurate AFM ordering of the Ho^{3+} moments and the c-axis modulated peaks appear at lower temperatures [24]. This means that both the ferromagnetic (FM) correlation of Ho^{3+} moments within the Ho–C plane and the AFM coupling between these layers are weakened. Our previous studies on the superconducting properties of $Ho_{1-x}Y_xNi_2B_2C$ ($x = 0.025$, 0.5, and 0.75) single crystals also show that T_c increases with increasing Y content while T_N decreases, which implies the strong magnetic pair-breaking effect of Ho^{3+} moments [25]. From the comparison of the magneto-resistivity curves for $\mathbf{H} \parallel c$ and $\mathbf{H} \perp c$ shown in the inset of figure 2(b), it can be easily seen that superconductivity is completely destroyed by the in-plane magnetic field in the region where reentrant behaviour occurs for $\mathbf{H} \parallel c$. $H_{c2}^{\perp}(T)$ is very close to H_P. Further studies including the details of magnetic structure in this system are necessary to understand the interplay between superconductivity and magnetic order.

4. Conclusion

The reentrant behaviour of $Ho_{0.75}Y_{0.25}Ni_2B_2C$ single crystals which experience a superconducting transition at T_c of 7.6 K and an AFM transition at T_N of 3.9 K was studied. In contrast to the case of $HoNi_2B_2C$, the reentrant behaviour for $Ho_{0.75}Y_{0.25}Ni_2B_2C$ single crystals is only observed for $\mathbf{H} \parallel c$. The reentrance into normal state happens at temperatures much above the AFM transition temperature T_N, and the reentrant peak shifts to lower temperatures with increasing magnetic field. Moreover, there does not exist a minimum in $H_{c2}(T)$ around T_N for either $\mathbf{H} \parallel c$ or $\mathbf{H} \perp c$. We suggest that the effect of the disorder induced by Y doping may account for the difference in the reentrant behaviour between $Ho_{0.75}Y_{0.25}Ni_2B_2C$ and $HoNi_2B_2C$. The H–T phase diagram is derived and discussed.

Acknowledgments

This work was supported by the National Natural Science Foundation of China (Grant No 10225417), the National Basic Research Program of China (Grant No 2006CB601003), and the Japan Society for the Promotion of Science.

References

[1] Cava R J *et al* 1994 *Nature* **367** 252
[2] Nagarajan R *et al* 1994 *Phys. Rev. Lett.* **72** 274
[3] Canfield P C 1998 *Phys. Today* **51** 40
[4] Muller K H and Narozhnyi V N 2001 *Rep. Prog. Phys.* **64** 943
[5] Cho B K *et al* 1995 *Phys. Rev.* B **52** 3676

[6] Cho B K *et al* 1995 *Phys. Rev.* B **52** 3684
[7] Krutzler C *et al* 2005 *Phys. Rev.* B **72** 144508
[8] Grigereit T E *et al* 1994 *Phys. Rev. Lett.* **73** 2756
[9] Huang Q *et al* 1995 *Phys. Rev.* B **51** 3701
[10] Eversmann K *et al* 1996 *Physica* C **266** 27
[11] Krug K *et al* 1996 *Physica* C **267** 321
[12] Dewhurst C D *et al* 1999 *Phys. Rev. Lett.* **82** 827
[13] Rathnayaka K D D *et al* 1996 *Phys. Rev.* B **53** 5688
[14] Lin M S *et al* 1995 *Phys. Rev.* B **52** 1181
[15] Amici A *et al* 2000 *Phys. Rev. Lett.* **84** 1800
[16] Goldman A I *et al* 1994 *Phys. Rev.* B **50** R9668
[17] Muller K H *et al* 1997 *J. Appl. Phys.* **81** 4240
[18] Takeya H and EI Massalami M 2004 *Phys. Rev.* B **69** 024509
[19] Takeya H *et al* 1996 *Physica* C **256** 220
[20] Rathnayaka K D D *et al* 1997 *Phys. Rev.* B **55** 8506
[21] Bhatnagar A K *et al* 1997 *Phys. Rev.* B **56** 437
[22] Maple M B and Fischer O 1982 *Superconductivity in Ternary Compounds III* (Berlin: Springer)
[23] Machida K *et al* 1980 *Phys. Rev.* B **22** 2307
[24] Chang L J *et al* 1996 *Physica* B **223/224** 119
[25] Zhao S R *et al* 2006 *Chin. Phys. Lett.* **23** 975